Photopatterning Using a Cross-Linkable Polymer Langmuir−Blodgett Film

Atsushi Aoki, Masakazu Nakaya, and Tokuji Miyashita*

Institute for Chemical Reaction Science, Tohoku University, Katahira 2-1-1, Aoba-ku, Sendai 980-8577, Japan

Received June 17, 1998; Revised Manuscript Received August 24, 1998

ABSTRACT: A cross-linkable amphiphilic copolymer of *N*-dodecylacrylamide with *N*-(11-acryloylundecyl)-4-vinylpyridinium bromide was prepared. This polymer when spread on a water surface forms a stable condensed monolayer that was transferred onto a solid support to yield a Langmuir−Blodgett (LB) film. On UV light irradiation, the polymer LB film became insoluble in all organic solvents because of the formation of a two-dimensional photo-cross-linked polymer network. The cross-linking reaction was found to be caused by dimerization of acryloyl groups in the LB film. Fine negative resist patterns based on the insoluble two-dimensional polymer network can be drawn clearly after development of irradiated LB films with a solvent. The patterns of the cross-linked polymer LB films of various film thicknesses from bilayer to 200 layers were successfully achieved by using a conventional photolithographic technique. The bilayer patterns of cross-linked polymer LB films were observed using atomic force microscopy (AFM). These films had a thickness of 1.0 nm and a uniform surface.

Introduction

Ultrafine patterning of LB films and self-assembled monolayers (SAMs) using electron beams,[1] UV light,[2,3] X-ray irradiation,[4] and scanning tunneling microscopy (STM)[5] have been greatly investigated in molecular engineering, ultrahigh-resolution lithography, and nanotechnology fields. There are two main aspects to realizing high-resolution patterning: One of these is the lithographic technique, which has been studied using deep UV light, X-rays, electron beams, and so on. The application of STM is a new technique for ultrafine patterning development. The second aspect is finding suitable lithographic materials. Instead of conventional spin-coated polymer films, more elaborate films such as LB films and SAMs have been employed. SAMs using alkanethiols[6,7] and organic silanes[8,9] have often been employed to draw ultrafine patterning because a well-defined monolayer on substrates with self-organization properties can be easily fabricated. Whitesides and coworkers presented the molecular stamping method using alkanethiol to a gold substrate.[6] Crooks and coworkers reported the polymeric self-assembling monolayers of diacetylenic alkanethiol using UV light irradiation.[7] Monolayer immobilization of receptors, antibodies, and other macromolecules by photoreaction of nitroveratryloxycarbonyl groups[8] and aryl azides with secondary amines[9] has also been reported.

The application of LB films to photolithography is expected to allow high-resolution patterning because of their molecularly ordered structure and ultrathin film thickness properties.[2,10,11] LB films have some advantages for the control of film thickness at a molecular level and compared to SAM cases, no substrate selection is required. Polymerization of monomer LB films by UV or electron beam irradiation techniques produces an insoluble polymerized LB film. As a result of polymerization, fine negative resist patterns can be drawn. A large difference in solubility between monomer and polymer LB films is one of the key factors in realizing the fine patterning. Since monomer molecules in LB films are known to align in a highly ordered orientation, nanoscale resolution is theoretically possible by quantitative and efficient polymerization. Polymerization of various monomer LB films has been studied with the aim of applying these films to a high-resolution negative resist. However, high degrees of polymerization in the solid state is generally difficult to achieve because of defects, grain boundaries, and crystallization of monomer LB films. A few successes in fine patterning using polymerization of monomer LB films have been found in films of ω-tricosenoic acid[12] and *N*-octadecylacrylamide.[13,14]

Recently, we have succeeded in the preparation of a preformed polymer LB film containing a cross-linkable group, which produces a two-dimensional network polymer LB film by cross-linking when irradiated with UV light.[15−18] In the linear polymer main chains of the LB film, only a small degree of cross-linking reaction produces an insoluble film. This results in higher sensitivity of the photolithography compared with those of monomer LB films. Polymer LB films have received much attention because of their stable thermal and mechanical properties compared with conventional LB films such as long alkyl chain fatty acids. We reported previously that preformed *N*-dodecylacrylamide (DDA) polymers have excellent spreading behavior and form stable polymer LB films.[19] Furthermore, we have also succeeded in the introduction of various functional groups such as redox species,[20] aromatic chromophores,[21] and chiral groups[22] into the polymer LB films as a comonomer of DDA. A few examples of cross-linkable polymer LB films, for example, poly(styrene-*co*-maleic anhydride) derivatives[23] for electron beam resists, poly(vinylpyridine) derivatives[24] for patterning, and poly(vinyl acetal)[25] and polyglutamate derivatives[26] for thermal stability, have been reported. No reports on molecular patterning using cross-linkable polymer LB films are available in the literature to date.

In the present study, our aim was to fabricate ultrafine patterning using cross-linkable polymer LB films. In bilayer LB films, photopatterning was confirmed by AFM. In addition, the cross-linking reaction

10.1021/ma980957a CCC: $15.00
Published on Web 10/03/1998

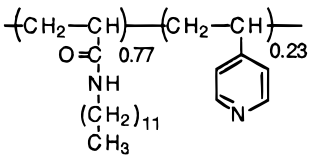

copolymer **1**

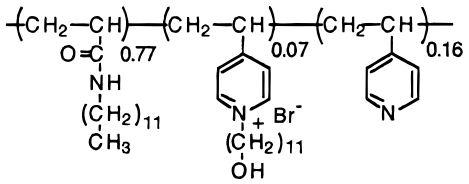

copolymer **2**

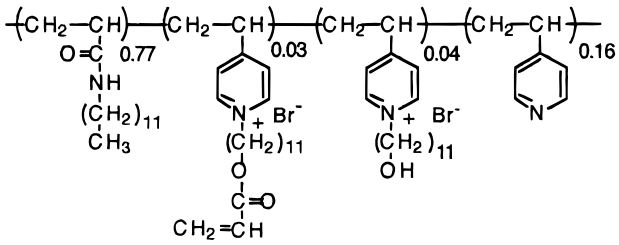

copolymer **3**

Figure 1. Chemical structures of copolymers **1**, **2**, and **3**.

mechanism with UV light irradiation and the orientation of cross-linkable groups in the monolayer and LB films were also investigated.

Experimental Section

Materials. The synthesis of a cross-linkable amphiphilic polymer, consisting of *N*-dodecylacrylamide (DDA) copolymer with *N*-(11-acryloylundecyl)-4-vinylpyridinium salt, was carried out by the same method described in a previous study (Figure 1).[15] The DDA copolymer **1** containing 4-vinylpyridine (vpy) was prepared by free radical polymerization in toluene at 60 °C for 24 h with 2,2′-azobis(isobutyronitrile). The fraction of the vpy moiety in the resulting copolymer **1** was quaternized with 11-bromo-1-undecanol under reflux in 2-propanol for 48 h. Copolymer **3** was obtained by reacting acryloyl chloride with the hydroxyl groups in the quaternized copolymer **2** in the presence of triethylamine in chloroform at room temperature. Copolymer **3** was washed with water to remove unreacted acryloyl chloride and triethylamine and then purified twice by precipitation from chloroform solution into a large excess of acetonitrile. The mole fractions of the copolymers were determined by ^{1}H NMR spectroscopy. Gel permeation chromatography analysis of copolymer **1** shows $M_n = 3.2 \times 10^4$ and $M_w/M_n = 2.1$. All other chemicals were of reagent grade and used without further purification.

General Methods. The measurement of surface pressure (π)−area (A) isotherms and deposition of the monolayers were carried out with a computer-controlled Langmuir trough FSD-11 (USI) at 20 °C. Distilled and deionized water (Millipore Milli-Q) was used for the subphase. Chloroform was used as a solvent for spreading the monolayer on the water surface. A quartz substrate and silicon wafer (100) were employed as a substrate for the monolayer. The quartz substrate was cleaned by immersing in a methanol solution containing 5 wt % KOH, boiling in dilute HNO_3 solution, and washing with pure water. Both substrates were subsequently treated with 2.0 vol % trimethylchlorosilane in chloroform for 1 h to make the substrate surface hydrophobic. After hydrophobic treatment, the substrates were cleaned by washing with chloroform, acetone, and water, respectively, to remove unreacted trimethylchlorosilane from the substrate surface. The monolayers of the copolymer were transferred onto these substrates by the vertical dipping method at a dipping speed of 10 mm min^{-1} and surface pressure of 35 mN m^{-1} at 20 °C.

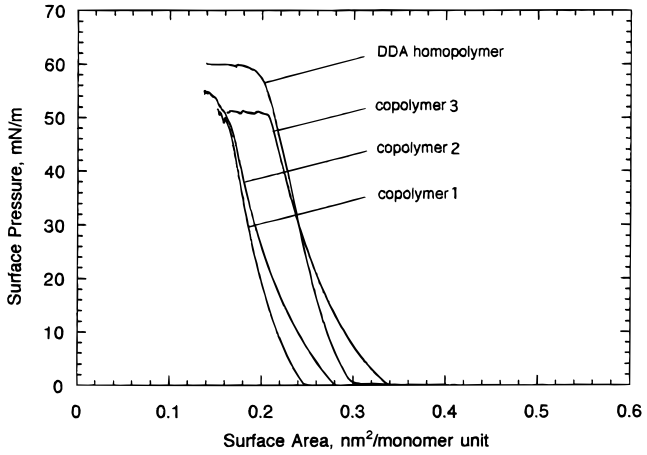

Figure 2. Surface pressure and molecular area isotherms of copolymers **1**, **2**, **3**, and *N*-polydodecylacrylamide at 20 °C.

UV absorption spectra were measured with a Hitachi UV−vis absorption spectrometer. X-ray diffraction (XRD) patterns were measured by using an X-ray diffractometer (Rigakudenki RAD-C). The copolymer LB films with 20 layers were employed for the XRD measurements.

Photopatterning. The cross-linkable copolymer LB films were irradiated for different times through a mask using a 500 W high-pressure mercury lamp (USHIO) filtered with a metal interference filter at 254 nm. The irradiated LB film was developed in chloroform for 10 s unless otherwise stated and dried with N_2 gas. The film thickness remaining after development as a function of exposure energy was determined with a Sloan DEKTAK ST surface profiler. The light intensity at the irradiating substrate surface was measured with an illuminance meter (TOPCON UVR-1) and the exposure energy was converted by multiplying the light intensity by the exposure time.

AFM Measurements. The photopattern image of the cross-linked polymer LB films were observed using a Nanoscope III microscope equipped with a 125 μm scan head (Digital Instrument).[27] All images were acquired in air in the contact mode using Si_3N_4 cantilevers with pyramidal tips at 35° cone angles and 20−40 nm nominal tip radii of curvature (R_c). Cantilevers with a force constant of 0.38 N/m were used to image LB films.

Results and Discussion

Monolayers of the Copolymers at the Air−Water Interface. The π−A isotherms of the copolymer monolayers on the water surface are shown in Figure 2. The collapse pressures of all copolymers were approximately 50 mN m^{-1}, indicating that the copolymers form a stable condensed monolayer on the water surface. The limiting molecular occupied surface areas obtained by extrapolation of the linear part of the π−A curve to zero surface pressure were different from each other. The limiting area of the copolymer **1** monolayer was smaller than that of the DDA homopolymer. Assuming that the additivity of the molecular area can hold in this system, the limiting area of the vpy moiety in copolymer **1** was calculated to be 0.02 nm^2 monomer unit^{-1}, which is smaller than the minimum area of the pyridine ring (0.16 nm^2) calculated from the CPK model. Since the

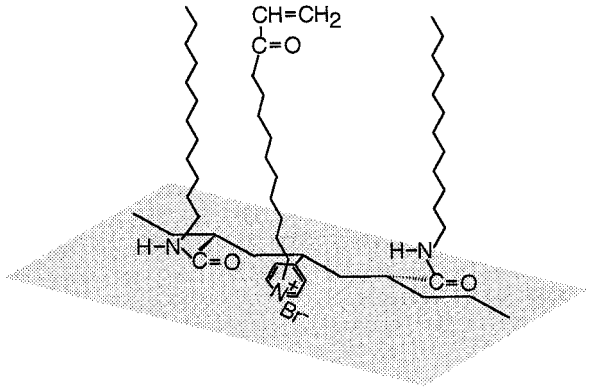

Figure 3. Schematic representation of the monolayer structure of copolymer **3** on a water surface.

pyridine moiety is hydrophilic, vpy in copolymer **1** appears to enter into the water subphase. The limiting area of the quaternized copolymer **2** is approximately the same as that of copolymer **1**. This result indicates that the quaternized pyridine ring, i.e., *N*-(11-hydroxyundecyl)pyridinium, is still held under the water surface because of the hydrophilic character of the quaternized pyridine. The *N*-(11-hydroxyundecyl)pyridinium moiety in copolymer **2** seems to be bolaamphiphile. On the other hand, the isotherm of copolymer **3**, which is synthesized by esterification of the hydroxy groups of copolymer **2** with acryloyl chloride shifts toward the larger surface area. By esterification of the hydroxyundecyl groups, part of the pyridinium substituent becomes hydrophobic and exists in its own surface area on the surface of the water. The limiting area of the acryloyl groups indicate that *N*-11-acryloylundecyl side chains stand perpendicular to the water surface and acryloyl groups are ordered on the hydrophobic plane in the monolayer on the water surface. We propose the orientation of the copolymer **3** monolayer on the water surface as illustrated in Figure 3.

The copolymer monolayers can be transferred onto substrates as a Y-type film with a transfer ratio of unity. The XRD patterns of copolymer **1** and **3** LB films are shown in Figure 4. One Bragg peak appears in both XRD patterns, suggesting a layered structure. The monolayer thickness was calculated to be 1.73 and 1.79 nm for copolymers **1** and **3**, respectively. As the monolayer thickness of the DDA homopolymer LB film was calculated to be 1.77 nm in a previous study,[23] the monolayer thickness will be slightly smaller in copolymer **1**, as incorporation of vpy into DDA polymer causes the dodecyl side chains to tilt. Meanwhile, the monolayer thickness of copolymer **3** becomes larger. These XRD results support the molecular orientation of copolymer **3** LB films suggested in Figure 3.

Photolithographic Properties of Copolymer 3 LB Films. The photolithographic property of copolymer **3** LB films was investigated by UV absorption spectroscopy and profilometry. Figure 5A shows UV absorption spectra for copolymer **3** LB films with 200 layers at different irradiation times. The results show that absorbances at wavelengths less than 270 nm decrease with irradiation time. It also appears that absorbances assigned to the acryloyl moieties (230 nm) and pyridinium rings (ca. 260 nm) decrease with irradiation time. To eliminate the influence of the pyridinium ring, the absorption spectra for copolymer **2** LB films with no acryloyl moiety were also measured at different irradiation times, as shown in Figure 5B. The difference

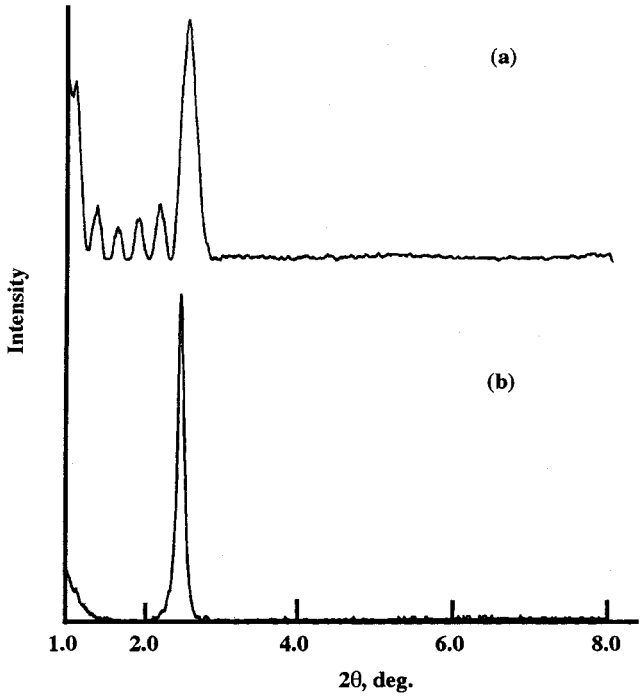

Figure 4. XRD patterns of copolymer **1** and **3** LB films with 20 layers on a silicon wafer: (A) copolymer **1**; (B) copolymer **3**.

between the absorption spectra of copolymer **3** and copolymer **2** LB films is shown in Figure 5C. The differential UV absorption spectra between LB films with and without acryloyl moieties show the absorbance at 230 nm due to the $\pi-\pi^*$ transition of the acryloyl groups, clearly decreases with irradiation time (Figure 5C). The surface concentration of acryloyl groups in the monolayer was calculated to be 1.9×10^{-11} mol cm^{-2} from the absorbance at 230 nm and the mole absorbance coefficient of acryloyl groups, i.e., 1.0×10^4 mol^{-1} dm^3 cm^{-1} [28] according to the following two-dimensional Lambert−Beer equation.

$$A = 1000\epsilon N\Gamma$$

where A is the absorbance, ϵ is the mole absorbance coefficient, N is the number of deposited layers, and Γ is the two-dimensional concentration per monolayer. Hence, one acryloyl group occupied an area of 8.7 nm^2. The absorbance at 230 nm was plotted according to first-order and second-order kinetics as shown in Figure 6. A linear plot is reasonably observed at second-order kinetics and absent at first-order kinetics in Figure 6. Therefore, the photoreaction in copolymer **3** LB films would appear to follow second-order kinetics. The dimerization of acryloyl groups can therefore be considered as the mechanism of the cross-linking reaction, as outlined in Figure 7.

In the UV absorption spectra of copolymer **2** LB films (Figure 5B), the absorbance at 260 nm assigned to the pyridinium moiety also decreases with irradiation time, indicating that the pyridinium moiety undergoes a photoreaction. The photoreaction of the pyridinium moiety may contribute to the insolubility of LB films in organic solvents. This point is discussed in detail later.

The solubility properties of copolymer **3** LB films in various organic solvents before and after irradiation with white light from a xenon lamp for 1 h are summarized in Table 1. Before irradiation, LB films

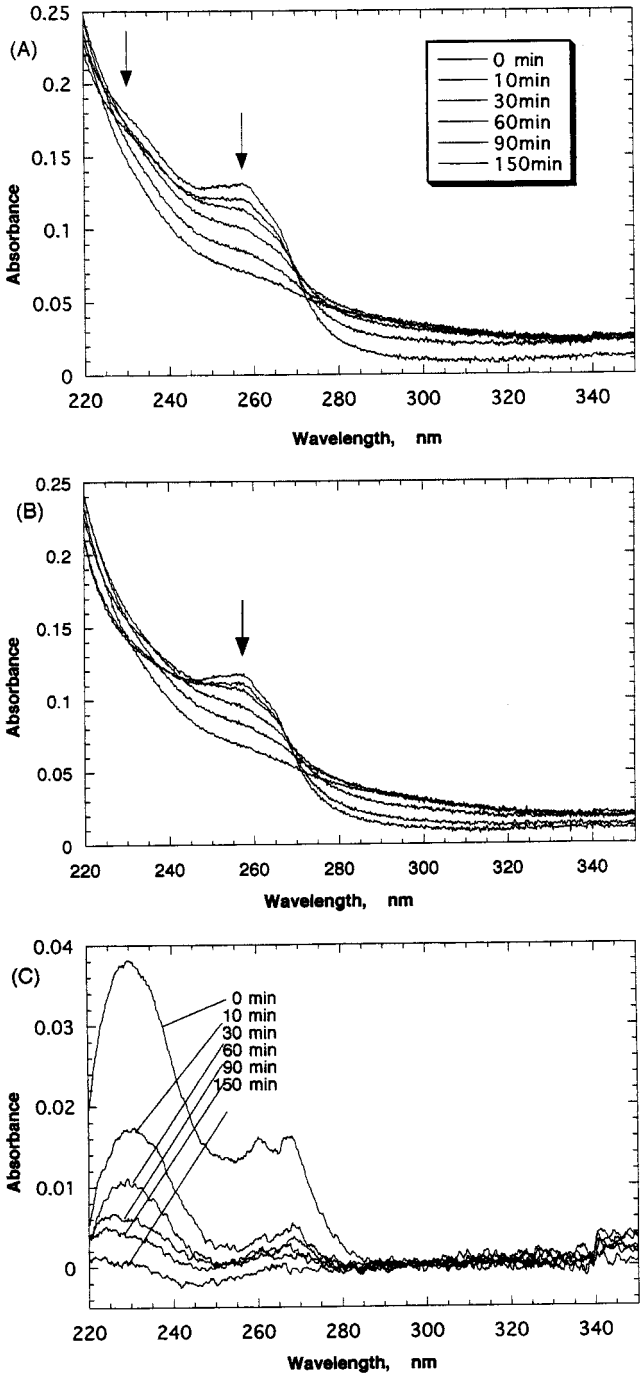

Figure 5. UV absorption spectra for the LB films with 200 layers on quartz substrates at different irradiating times: (A) copolymer **3** LB film; (B) copolymer **2** LB film; (C) difference between spectra (A) and (B). Wavelength of irradiation, 254 nm.

were highly soluble in halogenated solvents, toluene, THF, and ketone derivatives and insoluble in strong polar solvents such as DMF and acetone. This might be due to the amphiphilic nature of copolymer **3**; i.e., the main chain cannot be dissolved in polar solvents and pyridinium cations cannot be dissolved in nonpolar solvents. After irradiation, LB films were insoluble in all organic solvents used in this study. In a previous study, the photopolymerized *N*-octadecylacrylamide monomer LB film was found to be insoluble in many solvents but soluble in halogenated solvents.[13] The present strong resistance to organic solvents indicates that the linear polymer LB films are cross-linked at

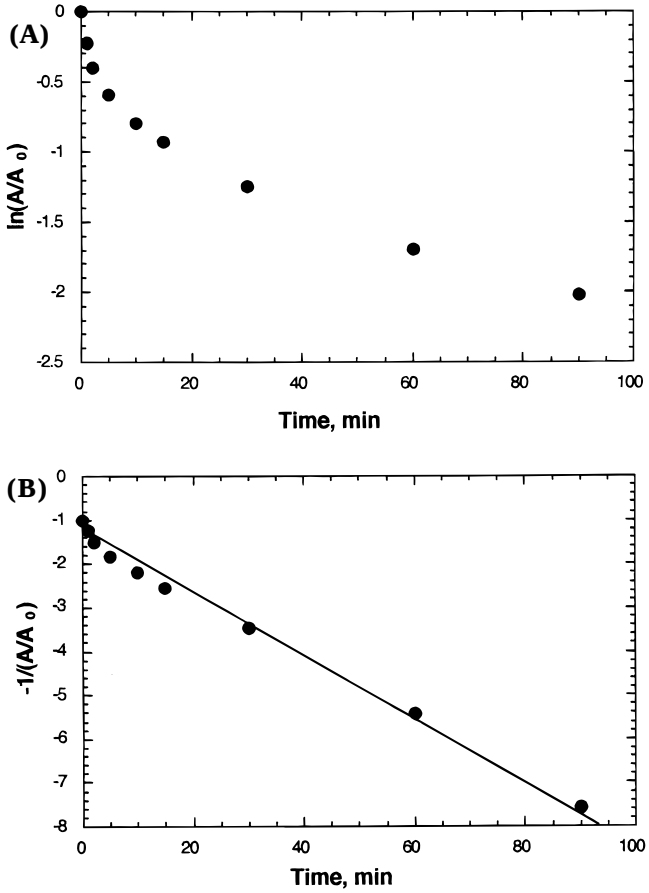

Figure 6. Relationship between absorbance at 230 nm and UV light irradiation time at 254 nm: (A) first-order kinetics; (B) second-order kinetics.

several points in the polymer chains, forming an insoluble two-dimensional polymer network.

It has been reported that some shrinkage and disorder caused by the reorientation of the LB film structure often occurs during photopolymerization of monomer LB films.[12] Figure 8 shows the XRD patterns of copolymer **3** LB films before and after irradiation and after solvent development. After UV light irradiation, one Bragg peak was still present in the XRD pattern at the same angle as that before irradiation. This result indicates that the LB film still has a layered structure with the layer distance being maintained after UV light irradiation. However, the LB films developed with the organic solvents do not have layered structures. Well-ordered alkyl side chains in the LB films are thought to become disordered in organic solvents.

After the development process, the normalized film thickness remaining was plotted as a function of the exposure energy in order to obtain a characteristic curve of the cross-linked polymer LB film, as shown in Figure 9. As all three copolymers became insoluble at high irradiation exposure energies, the cross-linking sites are thought to be the acryloyl groups and pyridine rings. The photographic sensitivity (D_{50}) was defined by the exposure energy at half the value of the film thickness.[29] However, the remaining normalized film thickness was 0.8 in copolymer **3** compared to 0.6 in copolymers **1** and **2**. Thus, the acryloyl group is a more effective cross-linkable moiety than the pyridine ring. The photographic contrast (γ) was determined from the initial slope of the characteristic curve,[29] and the photographic sensitivity and contrast of copolymer **1**, **2**, and **3** LB

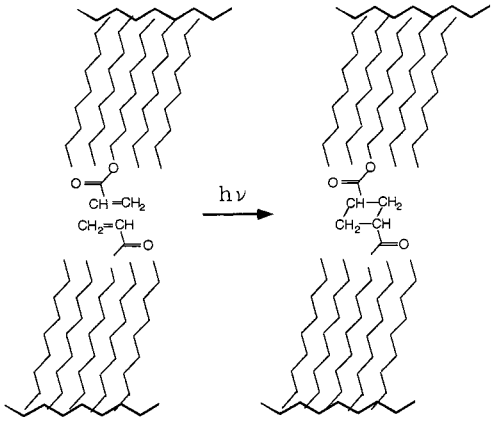

Figure 7. Schematic representation of the cross-linking reaction of acryloyl groups in the LB film: (A) interlayer cross-linking reaction; (B) in-plane cross-linking reaction.

Table 1. Comparison of Solubility between Nonirradiated and Irradiated Copolymer 3 LB Films in Various Solvents[a]

solvent	before irradiation	after irradiation
hexane, DMF, DMSO, acetone, acetonitrile, ethyl acetate, methanol	−	−
ethanol, dioxane, diglyme	+	−
2-propanol, methyl isobutyl ketone, diethyl ether, THF, dichloromethane, chloroform, *o*-dichlorobenzene, toluene	++	−

[a] −, insoluble; +, soluble; ++, highly soluble.

films with 40 layers are summarized in Table 2. The D_{50} value of copolymer **3** was determined to be 130 mJ cm^{-2}, 1 order of magnitude smaller than those of copolymers **1** and **2**. Therefore, it would appear that the cross-linking reaction of the pyridine ring is not a significant contributing factor to film insolubility during light irradiation of copolymer **3** films.

Photopatterning with Copolymer 3 LB Films. Ultrafine patterns of cross-linkable LB films with 40 layers and two layers were drawn using a photographic technique and observed using optical and atomic force microscopy, as shown in Figure 10. The optical microscopic observation in 40 layer LB films indicates that patterns can be drawn at a resolution of 0.75 μm line-and-space, which was the highest resolution of the photomask employed in this study. The surface structure from these patterns was observed to be uniform with no cracks evident, indicating that any shrinkage of the LB films caused by a cross-linking reaction and any swelling of the LB films following development with organic solvents are negligible. It is of interest that patterns of bilayer LB films are obviously evident in the AFM image at a resolution of 5.0 μm width, as indicated

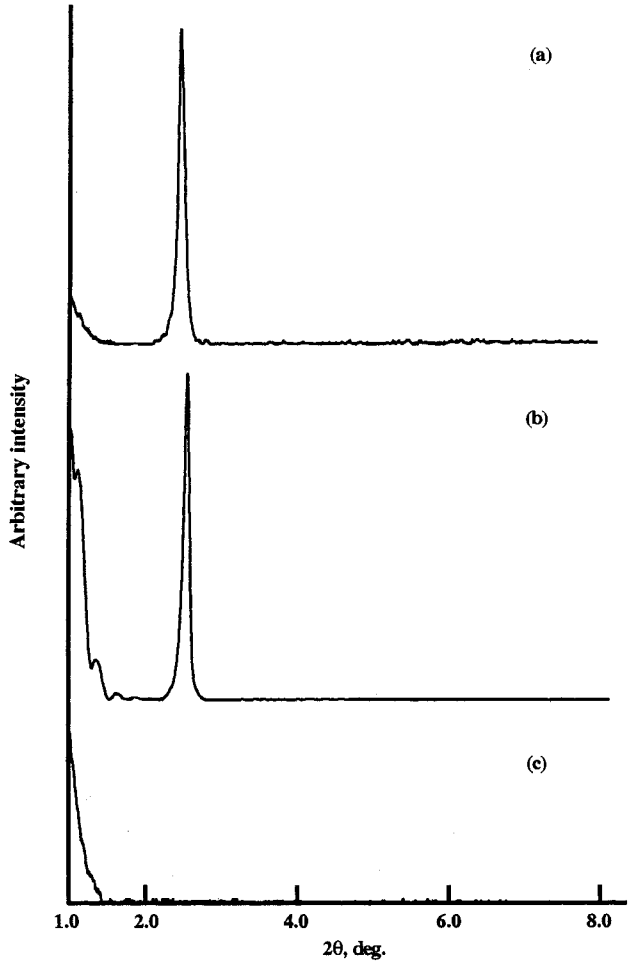

Figure 8. XRD patterns of copolymer **3** LB films with 20 layers on a silicon wafer: (A) before UV light irradiation; (B) after UV light irradiation; (C) after development.

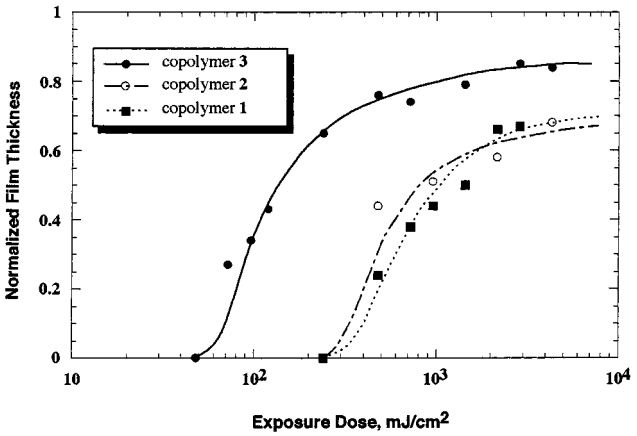

Figure 9. Sensitivity curves for copolymer **1**, **2**, and **3** LB films with 40 layers. Wavelength, 254 nm.

Table 2. Photographic Sensitivity and Contrast of Copolymer 1, 2, and 3 LB Films with 40 Layers

	sensitivity, mJ cm^{-2}	contrast
copolymer **1**	1000	1.0
copolymer **2**	800	1.4
copolymer **3**	130	1.7

by white areas in Figure 10B. The line surface is generally smooth except for several small holes and copolymer **3** residue dissolved during the development process also being observed. This indicates that the

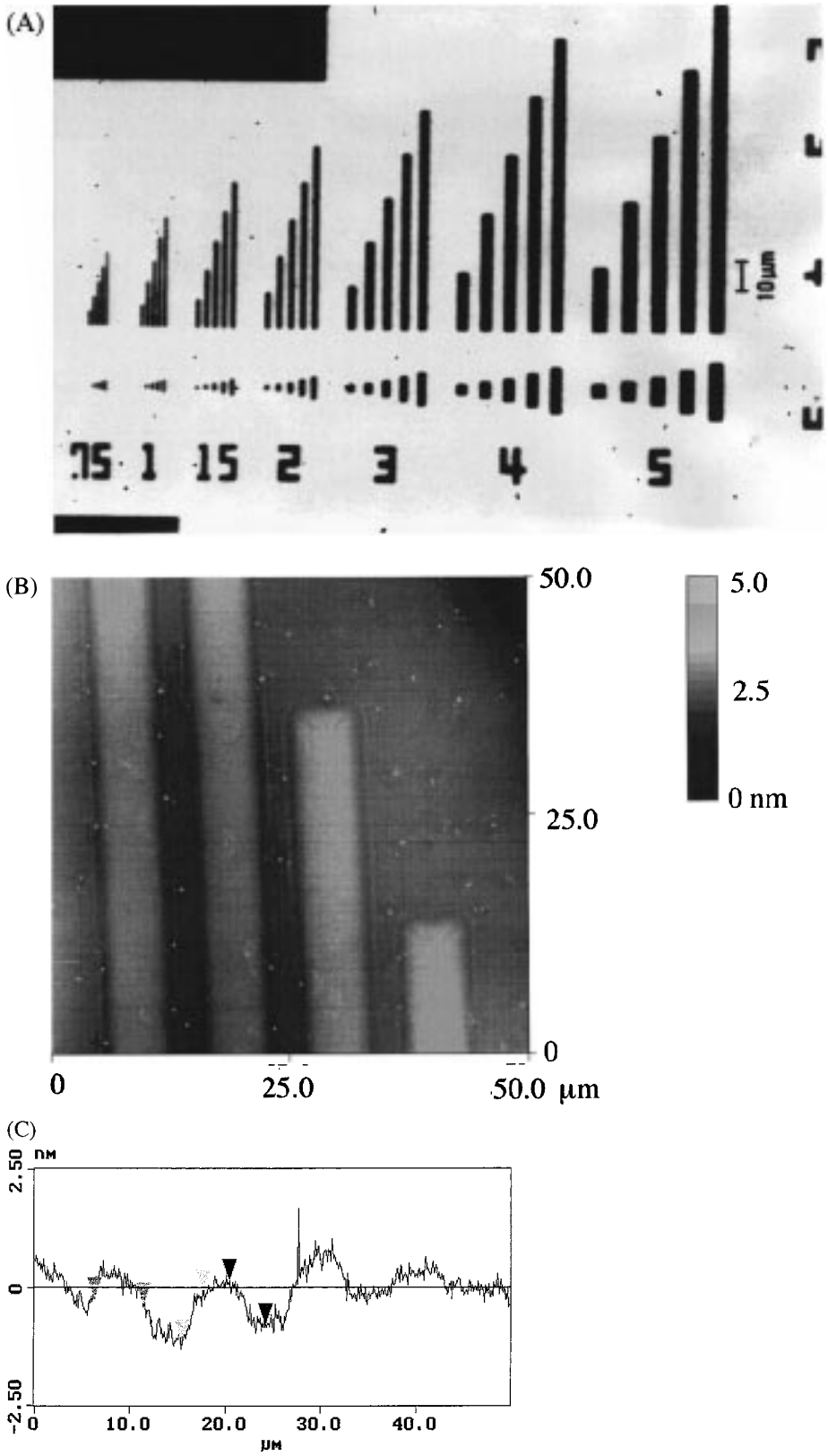

Figure 10. Photopatterns of two-dimensional polymer LB films: optical micrograph (A) for copolymer **3** LB films with 40 layers; AFM image (B) and AFM cross section (C) for copolymer **3** LB films with bilayer on a silicone wafer.

photo-cross-linking reaction almost occurs uniformly and the two-dimensional polymer network is also formed in the bilayer LB film. A number of dots attributed to the residue of dissolved copolymer **3** aggregates were observed in the dark area of the silicon wafer surface. The cross section of patterned copolymer **3** LB film is illustrated in Figure 10C. The film thickness of approximately 1.0 nm was determined from a cross section of the AFM image. The film thickness was much smaller than the film thickness of the bilayer LB film (3.58 nm), as calculated from XRD data. This apparent decrease in film thickness might be caused by the

development process of copolymer **3** LB films. That is, the layered structure of the LB film is destroyed after development because the order of the alkyl side chains in copolymer **3** are distorted by the developing solvent. The photolithographic resolution of the bilayer system (1.5 μm line-and-space, not shown in this paper) was not high at this stage because the conventional contact mask method was used and the irradiating condition and developing time were not optimized. Therefore, LB films developed during our investigation are potential candidates for high-resolution resist in nanolithography techniques.

In conclusion, cross-linkable groups are ordered on the hydrophobic plane in copolymer LB films. The ordered structure results in an efficient cross-linking reaction by dimerization of the acryloyl groups. Two-dimensional polymer network LB films can be constructed by UV light irradiation of the cross-linkable polymer LB films. Photopatterning of bilayer cross-linked polymer LB films was demonstrated. These cross-linkable polymer LB films are expected to be widely applicable in the construction of two-dimensional polymer LB films with stable thermal and mechanical properties, molecular patterning, and two-dimensional control of functional LB films.

Acknowledgment. This work was partially supported by the "Research for the Future" Program (JSPS-RFTF97P00302) from the Japan Society for the Promotion of Science. We would like to thank Dr. Tomokazu Matsue for use of the atomic force microscope in the center for interdisciplinary research. We would also like to thank Dr. Yasuo Ando for his help with film thickness and XRD measurements.

References and Notes

(1) (a) Lercel, M. J.; Tiberio, R. C.; Chapman, P. F.; Craighead, H. G.; Sheen, C. W.; Parikh, A. N.; Allara, D. L. *J. Vac. Sci. Technol. B* **1993**, *11*, 2823. (b) Lercel, M. J.; Redinbo, G. F.; Pardo, F. D.; Rooks, M.; Tiberio, R. C.; Simpson, P.; Craighead, H. G.; Sheen, C. W.; Parikh, A. N.; Allara, D. L.; *J. Vac. Sci. Technol. B* **1994**, *12*, 3663.

(2) Ulman, A. *An Introducion to Ultrathin Organic Films from Langmuir−Blodgett to Self-Assembly*; Academic Press: San Diego, 1991; p 391.

(3) Calvert, J. M. In *Thin Films*; Ulman, A., Ed.; Academic Press: San Diego, 1995; Chapter 6.

(4) Ogawa, K.; Tamura, H.; Hatada, M.; Ishihara, T. *Langmuir* **1988**, *4*, 1229.

(5) (a) Xu, L. S.; Allee, D. R. *J. Vac. Sci. Technol. B* **1995**, *13*, 2837. (b) Sugimura, H.; Nakagiri, N. *J. Am. Chem. Soc.* **1997**, *119*, 9226. (c) Schoer, K. J.; Zamborini, F. P.; Crooks, R. M. *J. Phys. Chem.* **1996**, *100*, 11086. (d) Schoer, K. J.; Crooks, R. M. *Langmuir* **1997**, *13*, 2323. (e) Nyffenegger, R. M.; Penner, R. M. *Chem. Rev.* **1997**, *97*, 1195.

(6) (a) Kumar, A.; Whitesides, G. M. *Appl. Phys. Lett.* **1993**, *63*, 2002. (b) Kumar, A.; Whitesides, G. M. *Science* **1994**, *263*, 60. (c) Kumar, A.; Biebuyck, H. A.; Whitesides, G. M. *Langmuir* **1994**, *10*, 1498.

(7) (a) Kim, T.; Crooks, R. M. *Tetrahedron Lett.* **1994**, *35*, 9501. (b) Chan, K. C.; Kim, T.; Schoer, J. K.; Crooks, R. M. *J. Am. Chem. Soc.* **1995**, *117*, 5875. (c) Kim, T.; Crooks, R. M.; Tsen, M.; Sun, L. *J. Am. Chem. Soc.* **1995**, *117*, 3963. (d) Kim, T.; Ye, Q.; Sun, L.; Chan, K. C.; Crooks, R. M. *Langmuir* **1996**, *12*, 6065. (e) Kim, T.; Chan, K. C.; Crooks, R. M. *J. Am. Chem. Soc.* **1997**, *119*, 189.

(8) Sundberg, S. A.; Barrett, R. W.; Pirrung, M.; Lu, A. L.; Kiangsoontra, B.; Holmes, C. P. *J. Am. Chem. Soc.* **1995**, *117*, 12050.

(9) Wollman, E. W.; Kang, D.; Frisbie, C. D.; Lorkovic, I. V.; Wrighton, M. S. *J. Am. Chem. Soc.* **1994**, *116*, 4395.

(10) Hodge, P.; Davis, F.; Tredgold, R. H. *Philos. Trans. R. Soc. London A* **1990**, *330*, 153.

(11) Miyashita, T. *Prog. Polym. Sci.* **1993**, *18*, 263.

(12) (a) Barraud, A.; Rosilio, C.; R-Teixier, A. *J. Colloid Interface Sci.* **1977**, *62*, 509. (b) Barraud, A.; Rosilio, C.; R-Teixier, A. *Thin Solid Films* **1980**, *68*, 91. (c) Barraud, A.; Rosilio, C.; R-Teixier, A. *Thin Solid Films* **1980**, *68*, 99.

(13) (a) Miyashita, T.; Yoshida, H.; Murakata, T.; Matsuda, M. *Polymer* **1987**, *28*, 311. (b) Miyashita, T.; Yoshida, H.; Matsuda, M. *Thin Solid Films* **1987**, *155*, L11. (c) Miyashita, T.; Yoshida, H.; Matsuda, M. *Thin Solid Films* **1989**, *168*, L47. (d) Miyashita, T.; Mizuta, Y.; Matsuda, M. *Br. Polym. J.* **1990**, *22*, 329. (e) Miyashita, T.; Suwa, T. *Langmuir* **1994**, *10*, 3387.

(14) Fuchs, H.; Ohst, H.; Prass, W. *Adv. Mater.* **1991**, *3*, 10.

(15) Aoki, A.; Nakaya, M.; Miyashita, T. *Chem. Lett.* **1996**, 667.

(16) Aoki, A.; Miyashita, T. *Adv. Mater.* **1997**, *9*, 361.

(17) Miyashita, T.; Nakaya, M.; Aoki, A. *Thin Solid Films*, in press.

(18) Miyashita, T.; Nakaya, M.; Aoki, A. *Supramol. Sci.*, in press.

(19) Mizuta, Y.; Matsuda, M.; Miyashita, T. *Langmuir* **1993**, *9*, 1158.

(20) (a) Aoki, A.; Miyashita, T. *Macromolecules* **1996**, *29*, 4662. (b) Aoki, A.; Miyashita, T. *Chem. Lett.* **1996**, 563.

(21) (a) Mizuta, Y.; Matsuda, M.; Miyashita, T. *Macromolecules* **1991**, *24*, 5459. (b) Miyashita, T.; Yatsue, T.; Matsuda, M. *J. Phys. Chem.* **1991**, *95*, 2448. (c) Yatsue, T.; Miyashita, T.; Matsuda, M. *J. Phys. Chem.* **1992**, *96*, 10125.

(22) Qian, P.; Matsuda, M.; Miyashita, T. *J. Am. Chem. Soc.* **1993**, *115*, 5624.

(23) Jones, R.; Winter, C. S.; Tredgold, R. H.; Hodge, P.; Hoorfar, A. *Polymer* **1987**, *28*, 1619.

(24) Davis, F.; Hodge, P.; Liu, X.-H.; Ali-Adib, Z. *Macromolecules* **1994**, *27*, 1957.

(25) (a) Ito, S.; Ueno, T.; Yamamoto, M. *Thin Solid Films* **1992**, *210/211*, 614. (b) Hayashi, T.; Mabuchi, M.; Mitsuishi, M.; Ito, S.; Yamamoto, M.; Knoll, W. *Macromolecules* **1995**, *28*, 2537.

(26) Mathauer, K.; Schmidt, A.; Knoll, W.; Wegner, G. *Macromolecules* **1995**, *28*, 1214.

(27) Caldwell, W. B.; Campbell, D. J.; Chen, K.; Herr, B. R.; Mirkin, C. A.; Malik, A.; Durbin, M. K.; Dutta, P.; Huang, K. G. *J. Am. Chem. Soc.* **1995**, *117*, 6071.

(28) Silverstein, R. M.; Bassler, G. C.; Morrill, T. C. *Spectrometric Identification of Organic Compounds*; John Wiley & Sons: New York, 1991; Chapter 7.

(29) (a) Reiser, A. *J. Chim. Phys.* **1980**, *77*, 469. (b) Reiser, A.; Pitts, E. *J. Photograph. Sci.* **1981**, *29*, 187.

MA980957A